J|A|C|S
ARTICLES
Published on Web 06/28/2002

# Structure of a Tethered Cationic 3-Aminopropyl Chain Incorporated into an Oligodeoxynucleotide: Evidence for 3′-Orientation in the Major Groove Accompanied by DNA Bending

Zhijun Li,[†] Li Huang,[†,§] Prasad Dande,[‡] Barry Gold,[‡] and Michael P. Stone*[,†]

*Contribution from the Department of Chemistry and Center in Molecular Toxicology, Vanderbilt University, Nashville, Tennessee 37235, and Eppley Institute for Research in Cancer and Allied Diseases and Department of Pharmaceutical Sciences, University of Nebraska Medical Center, Omaha, Nebraska 68198-6805*

Received February 4, 2002

***Abstract:*** The structure of the dodecamer d(CGCGAATXCGCG)$_2$, in which X = Z3dU, 5-(3-aminopropyl)-2′-deoxyuridine, was determined. At neutral pH, Z3dU introduced a positive charge into the major groove. NMR spectroscopy revealed that the Z3dU $\omega$-aminopropyl moiety oriented in the 3′-direction from the site of modification. Watson−Crick base pairing remained intact throughout the dodecamer. The presence of the charged amino group in the major groove resulted in a 0.24 ppm upfield shift of one $^{31}$P NMR resonance in the 3′-direction at the phosphodiester linkage between nucleotides C$^9$ and G$^{10}$. Molecular dynamics calculations restrained by distances obtained from $^1$H NOE data and torsion angles obtained from $^1$H NMR $^3J$ coupling data, and in which the $\omega$-amino group was constrained to be proximate to G$^{10}$O$^6$, predicted from the $^{31}$P NMR data and molecular modeling (Dande, P.; Liang, G.; Chen, F.-X.; Roberts, C.; Nelson, M. G.; Hashimoto, H.; Switzer, C.; Gold, B. *Biochemistry* **1997**, *36*, 6024−6032), were consistent with experimental NOEs. These refined structures exhibited bending. The distance from the amino group to the 5′-phosphate oxygen of Z3dU was >5 Å, which indicated that in this dodecamer the Z3dU amino group did not participate in a salt bridge to its 5′-phosphate.

The relationship between the electrostatic environment of DNA and its conformation is of considerable interest. The prevailing model posits that DNA conformation is controlled by a competition between base stacking, hydrogen bonding, and van der Waals interactions with electrostatic phosphodiester repulsion.[1,2] This predicts that asymmetric site-specific neutralization of phosphodiester charge results in collapse of the DNA backbone and induces DNA bending. Site-specific electrostatic interactions between regions of positive electrostatic potential in proteins and regions of negative electrostatic potential in the DNA duplex are associated with charge neutralization of the duplex and modulate bending.[3] If neutral methyl phosphonate residues are appropriately phased within sequences rich in C·G base pairs, at various distances from A-tracts, bending occurs. This has been attributed to neutralization of negative charge across the minor groove.[4]

The selective incorporation of nucleotides with cationic side chains into oligodeoxynucleotides allows the electrostatic potential of the double helix to be selectively perturbed. This substitution also induced DNA bending,[5] which was assigned to salt bridge formation via an electrostatic neutralization mechanism.[3,4,6,7] The substitution of pyrimidines with cationic side chains, e.g., 5-(6-aminohexyl)-2′-deoxycytidine, 5-(6-aminohexyl)-2′-deoxyuridine, or 5-(3-aminopropyl)-2′-deoxyuridine (Z3dU), into DNA generated regioselective inhibition of guanine N7 methylation by *N*-methyl-*N*-nitrosourea (MNU).[8,9] The inhibitory effect extended beyond the physical length of the aliphatic tether. This was consistent with the notion that the cationic moiety induced DNA bending. The footprinting studies suggested that the aminoalkyl side chain extended in the 3′-direction from the modified nucleotide. Molecular modeling also predicted 3′-orientation of the aminoalkyl group. This was based on unfavorable steric interactions in the 5′-direction. In addition, modeling predicted favorable electrostatic interac-

* To whom correspondence should be addressed. Phone: (615) 322-2589. Fax: (615) 322-7591. E-mail: stone@toxicology.mc.vanderbilt.edu.
[†] Vanderbilt University.
[‡] University of Nebraska Medical Center.
[§] Current address: Molecular Biology Core Facility, Meharry Medical College, Nashville, TN 37208.

(1) Manning, G. S. *Q. Rev. Biophys.* **1978**, *11*, 179−246.
(2) Manning, G. S.; Ebralidse, K. K.; Mirzabekov, A. D.; Rich, A. *J. Biomol. Struct. Dyn.* **1989**, *6*, 877−889.
(3) Mirzabekov, A. D.; Rich, A. *Proc. Natl. Acad. Sci. U.S.A.* **1979**, *76*, 1118−1121.
(4) Strauss, J. K.; Maher, L. J., III. *Science* **1994**, *266*, 1829−1834.
(5) Strauss, J. K.; Prakash, T. P.; Roberts, C.; Switzer, C.; Maher, L. J. *Chem. Biol.* **1996**, *3*, 671−678.
(6) Strauss, J. K.; Roberts, C.; Nelson, M. G.; Switzer, C.; Maher, L. J., III. *Proc. Natl. Acad. Sci. U.S.A.* **1996**, *93*, 9515−9520.
(7) Hardwidge, P. R.; Lee, D.; Prakash, T. P.; Iglesias, B.; Den, R. B.; Switzer, C.; Maher, L. J. *Chem. Biol.* **2001**, *8*, 967−980.
(8) Dande, P.; Liang, G.; Chen, F. X.; Roberts, C.; Nelson, M. G.; Hashimoto, H.; Switzer, C.; Gold, B. *Biochemistry* **1997**, *36*, 6024−6032.
(9) Heystek, L. E.; Zhou, H. Q.; Dande, P.; Gold, B. *J. Am. Chem. Soc.* **1998**, *45*, 12165−12166.

10.1021/ja0201707 CCC: $22.00 

***Chart 1.*** (A) Z3dU-Modified Dickerson Dodecamer[a] and (B) 5-(3-Aminopropyl)-2′-deoxyuridine and Designations of the Z3dU Protons

A

$$5'\text{-}C^{1}\ G^{2}\ C^{3}\ G^{4}\ A^{5}\ A^{6}\ T^{7}\ X^{8}\ C^{9}\ G^{10}C^{11}G^{12}\text{-}3'$$
$$3'\text{-}G^{12}C^{11}G^{10}C^{9}\ X^{8}\ T^{7}\ A^{6}\ A^{5}\ G^{4}\ C^{3}\ G^{2}\ C^{1}\ \text{-}5'$$

B

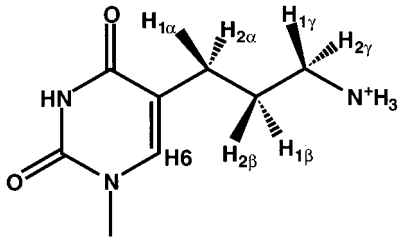


[a] X = 5-(3-aminopropyl)-2′-deoxyuridine.

tions with electronegative guanine $O^6$ and N7 atoms on the floor of the major groove of the DNA. On the other hand, the modeling predicted an absence of interactions between the cationic side chains and the phosphodiester backbone. Dande et al.[8] suggested that bending induced by cations tethered in the major groove arose by a mechanism proposed by Rouzina and Bloomfield.[10] In the model, cations bound in the major groove electrostatically repelled sodium ions from neighboring phosphates. The unscreened phosphates on both strands of the DNA were attracted to the cation, resulting in duplex bending toward the cation. This differed from a model in which bending was introduced by salt bridge formation between the aminoalkyl chain and the phosphodiester backbone.[4,5,7]

In this work, the tethered cation Z3dU has been introduced into the major groove of $d(CGCGAATXCGCG)_2$, the Dickerson−Drew dodecamer (Chart 1; X = Z3dU). The resulting Z3dU-modified dodecamer has been examined by NMR spectroscopy. The results confirm that the Z3dU $\omega$-aminopropyl moiety orients in the 3′-direction from the site of modification, and intact Watson−Crick base pairing is maintained. The charged amino group in the major groove results in an upfield shift of the $^{31}$P NMR resonance associated with the phosphodiester linkage between nucleotides $C^9$ and $G^{10}$. This is located in the 3′-direction from the site of the modification. Structural refinement using molecular dynamics calculations restrained by $^1$H NOE, $^3J$ coupling data, and $^{31}$P NMR data reveals that the distance from the $\omega$-amino group to the 5′-phosphate oxygen of Z3dU is >5 Å. Collectively, the data corroborate footprinting studies[9,11] that show that the Z3dU $\omega$-aminoalkyl side chain protects DNA from methylation toward the 3′-direction, with no evidence for salt bridge formation. Structures emergent from restrained molecular dynamics calculations in which the $\omega$-amino group is constrained to be proximate to $G^{10}O^6$, a location on the floor of the major groove predicted from molecular modeling,[8] are consistent with experimental NOEs. These refined structures exhibit bending.

## Experimental Section

**Sample Preparation.** The Z3dU-substituted oligodeoxynucleotide 5′-d(CGCGAATXCGCG)-3′ was synthesized[9] and was purified by HPLC using a reversed-phase semipreparative column (Phenomenex, Phenyl-Hexyl, 5 $\mu$m, 250 × 10.0 mm) equilibrated with 0.1 M ammonium formate (pH 7.0). The purified sample was characterized using multiple methods, including capillary gel electrophoresis and mass spectrometry. The self-complementary oligodeoxynucleotide was dissolved in 0.5 mL of buffer containing 0.1 M NaCl, 10 mM $NaH_2PO_4$, and 50 $\mu$M $Na_2EDTA$ at pH 7.0 in either 99.996% $D_2O$ or 90%:10% $H_2O$:$D_2O$ (for the observation of exchangeable protons). The oligodeoxynucleotide concentration was determined as ∼0.86 mM using an extinction coefficient of $1.10 \times 10^5$ $M^{-1}$ $cm^{-1}$ at 260 nm.[12]

**NMR Measurements.** All experiments were carried out at a $^1$H NMR frequency of 500.13 MHz. NMR data were processed using FELIX (v. 97.0, Accelyris, Inc., San Diego, CA) on Silicon Graphics (Mountain View, CA) Octane workstations. Chemical shifts of proton resonances were referenced to the water resonance, and trimethyl phosphate was used as an external standard for the $^{31}$P NMR chemical shifts. To derive the distance restraints from NOESY experiments, three spectra were recorded consecutively at mixing times of 150, 200, and 250 ms, respectively. In these experiments, the data were recorded with 1024 real data points in the *t*1 dimension and 2048 real points in the *t*2 dimension. The relaxation delay was 2 s. The data in the *t*1 dimension were zero-filled to give a matrix of 2K × 2K real points. A skewed sine-bell-square apodization function with a 90° phase shift and a skew factor of 1.0 was used in both dimensions.

**Generation of NOE and Torsion Angle Restraints.** Footprints were drawn around the NOE cross-peaks for the NOESY spectrum measured at a mixing time of 250 ms to define the size and shape of individual cross-peaks using FELIX. The same set of footprints was applied to spectra measured at other mixing times. Cross-peak intensities were determined by volume integration of the areas under the footprints. The intensities were combined with intensities generated from complete relaxation matrix analysis of a starting DNA structure to generate a hybrid intensity matrix.[13] MARDIGRAS (v. 5.2)[14,15] was used to refine the hybrid matrix by iteration to optimize the agreement with experimental NOE intensities. The molecular motion was assumed isotropic. Calculations were performed using the DNA starting models generated in INSIGHT II (v. 97.0, Accelyris, Inc., San Diego, CA), and using NOE intensities derived from experiments at three mixing times, and with three $\tau_c$ values (2, 3, and 4 ns). The noise level was set at half the intensity of the weakest cross-peak. The resulting sets of distances generated by 50 cycles of MARDIGRAS iteration were averaged to give the experimental NOE restraints used in subsequent molecular dynamics calculations. For partially overlapped cross-peaks, the lower and upper bounds on the distances were increased. The distance restraints were divided into four classes based on the quality of the NOE cross-peak (degree of overlapping). Pseudorotational angles (*P*) of the deoxyribose rings were estimated by examining the $^3J_{HH}$ of sugar protons as described by Salazar et al.[16] $J_{1'-2'}$ and $J_{1'-2''}$ were measured from the ECOSY experiment, while the intensities of cross-peak of H2″−H3′ and H3′−H4′ were examined from the DQF−COSY spectrum. A list of experimental distance restraints along with the upper and lower bounds is shown in the Table S1 in the Supporting Information.

**Additional Restraints.** A symmetry distance restraint function was used to restrain the distance difference to zero between two symmetric protons, based on the evidence that a fully degenerate set of cross-peaks was observed in the NOE spectra of the modified self-complementary dodecamer. Empirical base pair planarity restraints and Watson−Crick hydrogen-bonding restraints were used. The Watson−Crick hydrogen-bonding restraints were consistent with crystallographic

(10) Rouzina, I.; Bloomfield, V. A. *Biophys. J.* **1998**, *74*, 3152−3164.
(11) Liang, G.; Encell, L.; Nelson, M. G.; Switzer, C.; Gold, B. *J. Am. Chem. Soc.* **1995**, *117*, 10135−10136.
(12) Borer, P. N. *Handbook of biochemistry and molecular biology*; CRC Press: Cleveland, OH, 1975.
(13) Keepers, J. W.; James, T. L. *J. Magn. Reson.* **1984**, *57*, 404−426.
(14) Borgias, B. A.; James, T. L. *J. Magn. Reson.* **1990**, *87*, 475−487.
(15) Liu, H.; Tonelli, M.; James, T. L. *J. Magn. Reson. B* **1996**, *111*, 85−89.
(16) Salazar, M.; Fedoroff, O. Y.; Miller, J. M.; Ribeiro, N. S.; Reid, B. R. *Biochemistry* **1993**, *32*, 4207−4215.

data[17] and similar to those previously used in structural determination of oligodeoxynucleotides.[18,19] The inclusion of empirical restraints was based on NMR data that showed the modified DNA maintained Watson−Crick base pairing. The backbone torsion angles $\alpha$, $\beta$, and $\xi$ were loosely constrained to $-60° \pm 30°$, $180° \pm 30°$, and $-90° \pm 30°$, respectively, to maintain both A- and B-like geometry.[20]

**Structure Calculations.** A series of restrained molecular dynamics calculations using a simulated annealing protocol were performed using X-PLOR (v. 3.851).[21] Calculations were performed in vacuo without explicit counterions. The force field was derived from CHARMM[22] and adapted for restrained molecular dynamics (rMD) calculations of nucleic acids. The Z3dU partial charges were derived using MOPAC implemented in INSIGHT II (v. 97.0). The empirical energy function[22] consisted of terms for bonds, bond angles, torsion angles, tetrahedral and planar geometry, hydrogen bonding, and nonbonded interactions including van der Waals and electrostatic forces. It treated hydrogens explicitly. The van der Waals energy term used the Lennard-Jones potential energy function. The electrostatic term used the Coulomb function, based on a full set of partial charges (−1 per residue) and a distance-dependent dielectric constant of 4*r*. The nonbonded pair list was updated if any atom moved more than 0.5 Å, and the cutoff radius for nonbonded interactions was 11 Å. The effective energy function included terms describing distance and dihedral restraints, in the form of square-well potentials. Sets of rMD calculations were performed using two starting structures, a B-like model (ZdU-B) and an A-like model (ZdU-A), which were based on B-form and A-form DNA, respectively. Both were generated using INSIGHT II through modification of the methyl group of $T^7$, followed by energy minimization using X-PLOR. Calculations were initiated by coupling to a heating bath, with a target temperature of 1100 K. The force constants were 25 kcal mol$^{-1}$ Å$^{-2}$ for empirical hydrogen bonding, 10 kcal mol$^{-1}$ Å$^{-2}$ for torsion angle restraints, and 50, 45, 40, and 35 kcal mol$^{-1}$ Å$^{-2}$ for the four classes of NOE restraints. The target temperature was reached in 10 ps and was maintained for 25 ps. The molecules were cooled to 300 K over 10 ps and maintained at that temperature for 25 ps of equilibrium dynamics. The force constants for the four classes of NOE restraints were scaled up during 10 ps of the heating period to 200, 180, 160, and 140 kcal mol$^{-1}$ Å$^{-2}$ in the order of confidence factor. These weights were maintained during the remainder of the heating period and for the first 5 ps of the equilibrium dynamics period. They were then scaled down to 100, 90, 80, and 70 kcal/mol$^{-1}$ Å$^{-2}$ in the order of confidence factor. The torsion angle and base pair distance force constants were scaled up to 180 and 100 kcal mol$^{-1}$ Å$^{-2}$ during the same period as for the NOE restraints. They were scaled back to 70 and 45 kcal mol$^{-1}$ Å$^{-2}$, also at the same time as the NOE restraints. Coordinate sets were archived every 0.1 ps, and 41 structures from the last 4.1 ps were averaged. These average rMD structures were subjected to 700 iterations of conjugate gradient energy minimization to obtain the final structures. Final structures were analyzed using X-PLOR to measure rmsd between an average structure and the converged structures. Back-calculation of theoretical NMR intensities from the emergent structures was performed using CORMA (v. 5.2).[13] Structure rmsd was calculated using X-PLOR. The structures were analyzed using DIALS AND WINDOWS 1.0.[23]

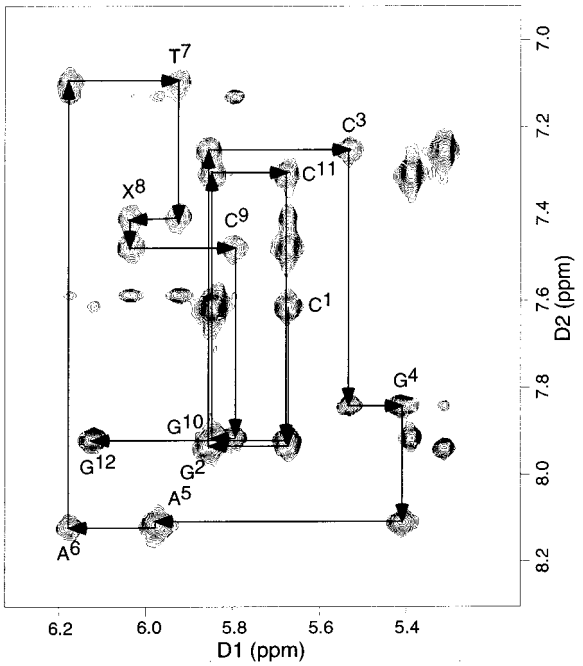


***Figure 1.*** Expanded plots from the aromatic−anomeric region of the 500.13 MHz NOESY spectrum at 10 °C using a 250 ms mixing time, showing sequential NOE connectivities.

## Results

**NMR Spectroscopy.** The modified dodecamer yielded well-resolved spectra. The pseudodyad symmetry of the dual Z3dU modifications (Chart 1) was evident. Overall, the spectrum of the Z3dU-modified dodecamer was similar to that of the unmodified dodecamer.[20,24] The presence of the cationic Z3dU residue had little effect on the $T_m$ of the modified dodecamer, as compared to the unmodified oligodeoxynucleotide.

**(a) DNA Protons.** Normal sequential NOE connectivities for base steps were observed for all bases, and no NOE peaks exhibited unusual intensities (Figure 1, Table S2 in the Supporting Information). The chemical shifts for the anomeric and the H6 aromatic resonances of the Z3dU-modified nucleotide were in the expected range. The imino protons of the Z3dU-modified dodecamer were assigned from NOE connectivities between adjacent base pairs and connectivities to the base-paired amino protons (Figure 2, Table S4 in the Supporting Information). The imino resonance of the Z3dU nucleotide, $X^8$, was observed at 13.9 ppm. It exhibited NOEs to $T^7$ N3H and to $G^4$ N1H of the complementary strand. All other imino protons except those from the terminal base pairs were observed without displaying significant changes in either their intensities or their chemical shifts.

**(b) Aminopropyl Protons of Z3dU.** Figure 3 shows an expanded region of the NOESY spectrum showing the assignment of the 3-aminopropyl side chain. The aminopropyl protons were assigned from a combination of NOESY, TOCSY, and DQF−COSY data. Resonances at 1.58 and 1.70 ppm were assigned to H$\beta$ protons on the basis of the cross-peak pattern to H$\alpha$ and H$\gamma$ protons in TOCSY and DQF−COSY spectra. The most downfield peak among 3-aminopropyl resonances was at 2.90 ppm and assigned to the H$\gamma$ proton adjacent to the

(17) Saenger, W. *Principles of Nucleic Acid Structure*; Springer: New York, 1984.
(18) Weisz, K.; Shafer, R. H.; Egan, W.; James, T. L. *Biochemistry* **1994**, *33*, 354−366.
(19) Tonelli, M.; Ragg, E.; Bianucci, A. M.; Lesiak, K.; James, T. L. *Biochemistry* **1998**, *37*, 11745−11761.
(20) Tjandra, N.; Tate, S.; Ono, A.; Kainosho, M.; Bax, A. *J. Am. Chem. Soc.* **2000**, *26*, 6190−6200.
(21) Brunger, A. T. *X-Plor. Version 3.1. A system for X-ray Crystallography and NMR*; Yale University Press: New Haven, CT, 1992.
(22) Nilsson, L.; Clore, G. M.; Gronenborn, A. M.; Brunger, A. T.; Karplus, M. *J. Mol. Biol.* **1986**, *188*, 455−475.
(23) Ravishankar, G.; Swaminathan, S.; Beveridge, D. L.; Lavery, R.; Sklenar, H. *J. Biomol. Struct. Dyn.* **1989**, *6*, 669−699.
(24) Hare, D. R.; Wemmer, D. E.; Chou, S. H.; Drobny, G.; Reid, B. R. *J. Mol. Biol.* **1983**, *171*, 319−336.

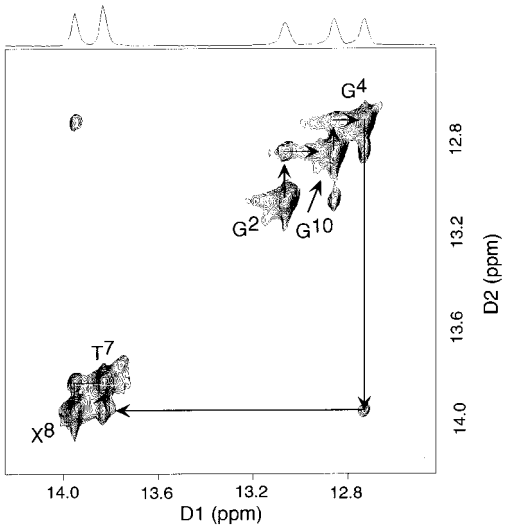


***Figure 2.*** Expanded plot showing sequential NOE connectivities for the imino protons of base pairs $G^2 \cdot C^{23} \rightarrow C^{11} \cdot G.^{14}$ The labels represent the imino proton of the designated base. Also shown is a 1D projection of the imino proton resonances. The 500.13 MHz NOESY spectrum was collected at 250 ms mixing time and 10 °C.

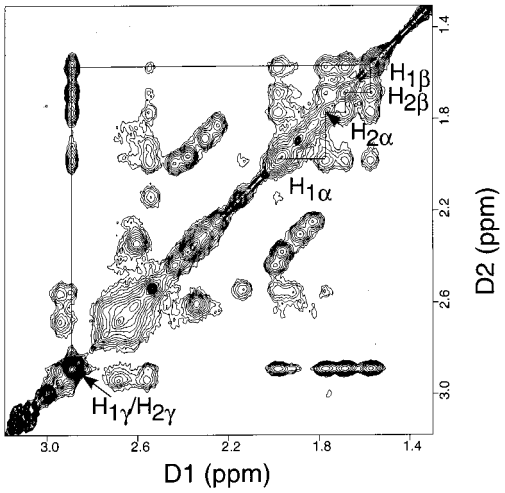


***Figure 3.*** Expanded 500.13 MHz NOESY spectrum at 250 ms mixing time showing the assignments for the 5-(3-aminopropyl) protons. The experiment was done at 10 °C. Protons H1$\gamma$ and H2$\gamma$ were not assigned specifically.

terminal amino group. Resonances at 1.98 and 1.78 ppm were assigned to H$\alpha$ protons. The DQF−COSY failed to show cross-peaks between resonances at 1.98 and 1.70 ppm, and between resonances at 1.78 and 1.58 ppm, suggesting their $^1$H NMR $^3J$ coupling constants were $< \sim 3$ Hz. Thus, spectroscopy predicted that the $H1_\alpha-C_\alpha-C_\beta-H2_\beta$ torsion angle was in the range of 90−120°, as was the $H2_\alpha-C_\alpha-C_\beta-H1_\beta$ torsion angle. Hence, the torsion angle $C_\alpha-C_\beta$ was concluded to adapt the conformation in which the uridine nucleobase and C$\gamma$ were in the trans orientation. In turn, this allowed stereotopic assignment of the prochiral protons attached to carbons $C_\alpha$ and $C_\beta$. The assignment of $\gamma$ protons could not be made specifically. The chemical shifts of the $\omega$-aminopropyl protons are listed in Table S3 in the Supporting Information.

**(c) Aminopropyl-DNA NOEs.** There were 19 NOEs observed between the $\omega$-aminopropyl moiety and DNA protons. These are shown in Figure 4. The observed pattern of NOEs placed the aminopropyl moiety into the major groove of the

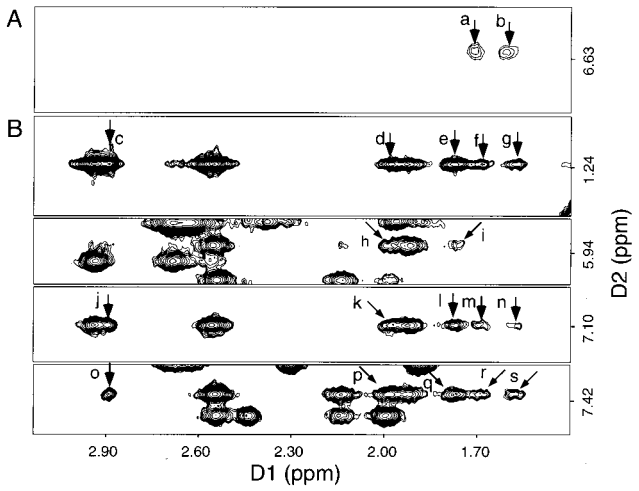


***Figure 4.*** Tile plot showing NOE cross-peaks between (A) exchangeable and (B) nonexchangeable protons of DNA and 5-(3-aminopropyl) protons. (a,b) $C^9$ non-hydrogen-bonded amino proton → Z3dU H2$\beta$ and H1$\beta$; (c−g) $T^7$ $CH_3$ → Z3dU H1$\gamma$/H2$\gamma$, H1$\alpha$, H2$\alpha$, H2$\beta$, and H1$\beta$; (h,i) $T^7$ H1′ → Z3dU H1$\alpha$ and H2$\alpha$; (j−n) $T^7$ H6 → Z3dU H1$\gamma$/H2$\gamma$, H1$\alpha$, H2$\alpha$, H2$\beta$, and H1$\beta$; (o−s) $X^8$ H6 → Z3dU H1$\gamma$/H2$\gamma$, H1$\alpha$, H2$\alpha$, H2$\beta$, and H1$\beta$.

duplex DNA, and helped establish the orientation of the $\omega$-ammonium group in the 3′-direction from $X^8$. The $H1_\alpha$ and $H2_\alpha$ protons showed stronger NOEs with $T^7$ $CH_3$ and H6 than did H1$\gamma$ and H2$\gamma$. Nucleotide $T^7$ is the 5′-neighbor of $X^8$. On the other hand, $H1_\beta$ and $H2_\beta$ but not $H1_\alpha$ and $H2_\alpha$ or H1$\gamma$ and H2$\gamma$ showed NOEs to the $C^9$ $N^4H$ exocyclic amino proton. Nucleotide $C^9$ is the 3′-neighbor of $X^8$. Therefore, the $H1_\alpha$,-$H2_\alpha$ and H1$\gamma$,H2$\gamma$ were oriented away from the DNA duplex, toward the solvent. In contrast, $H1_\beta$ and $H2_\beta$ were oriented toward the duplex and proximate to the exocyclic amino group of $C^9$.

**Chemical Shift Perturbations.** The $^1$H NMR chemical shifts of the modified dodecamer were compared with those of the unmodified dodecamer (Figure 5). No large deviations were observed, including protons on the modified base $X^8$. Figure 6 shows an expansion of the $^{31}$P HMBC spectrum, showing $^3J$ couplings between the phosphorus nuclei in the phosphodiester backbone and the deoxyribose H3′ protons. There was a 0.24 ppm upfield $^{31}$P NMR chemical shift observed for the phosphodiester linkage between $C^9$ and $G^{10}$. This was the second phosphodiester linkage in the 3′-direction from Z3dU. A smaller 0.10 ppm downfield chemical shift was noted for the phosphodiester linkage between $X^8$ and $C^9$, the first phosphodiester linkage in the 3′-direction from Z3dU. No significant chemical shift changes were observed for $^{31}$P NMR resonances arising from the other phosphodiester linkages. The $^{31}$P NMR data corroborated the NOESY data, suggesting that the Z3dU propylammonium side chain was oriented in the 3′-direction. The chemical shifts of the phosphate backbones are listed in Table S5 in the Supporting Information.

**Structural Refinement.** Structural refinement using restrained molecular dynamics calculations was conducted using the NOE-generated distance restraints augmented by an additional distance restraint that required the cationic Z3dU $\omega$-ammonium group to be proximate to the electronegative center at $G^{10}O^6$. The rationale for this additional restraint was the $^{31}$P NMR chemical shift perturbation at the phosphodiester linkage between $C^9$ and $G^{10}$. This chemical shift was interpreted to result from the proximity of the charged $\omega$-ammonium group

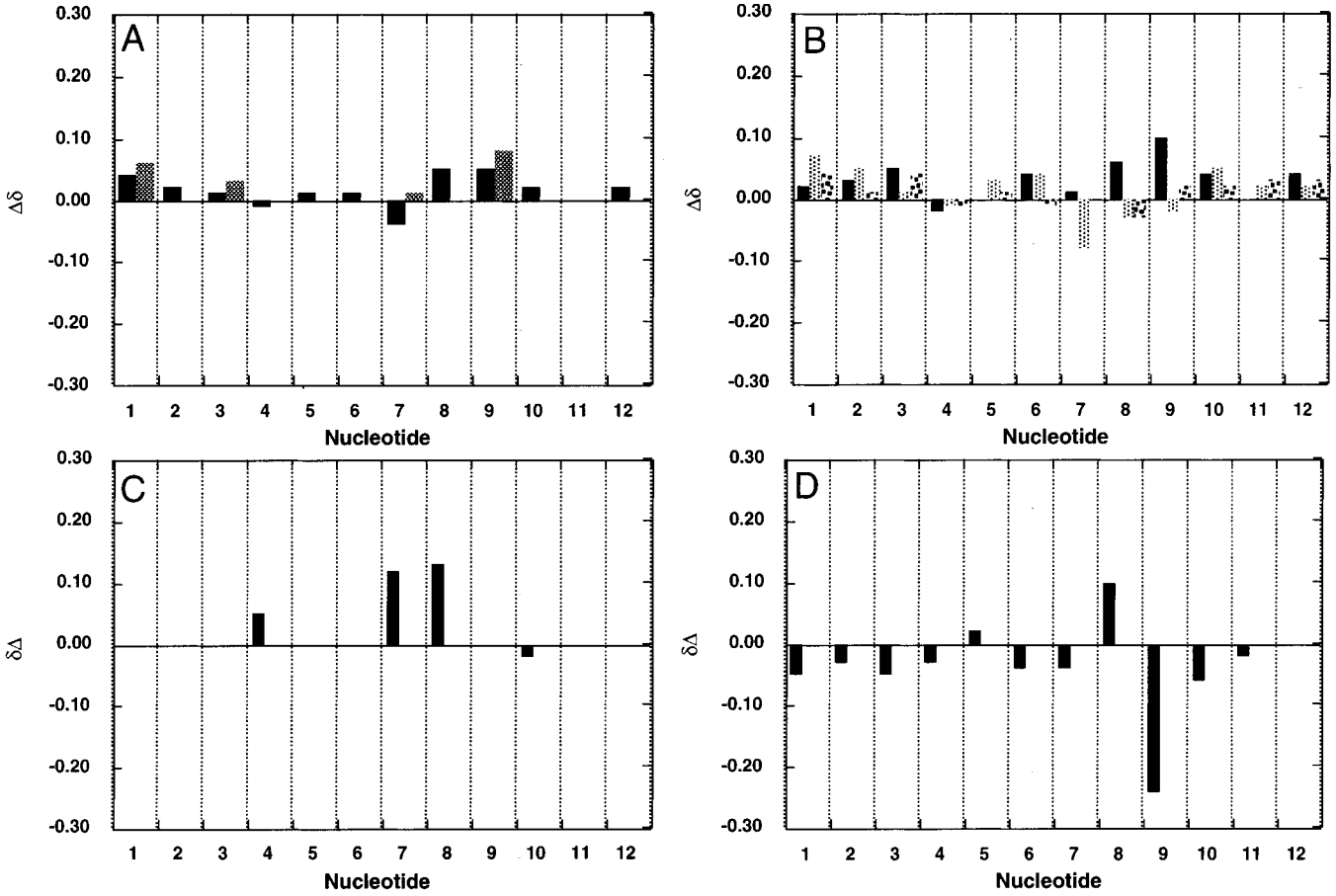


***Figure 5.*** Chemical shift changes of selected protons relative to the unmodified oligodeoxynucleotide duplex. (A) Major groove protons. Solid bars, G/A H8 or C/T H6; open bars, C H5 or T $CH_3$. (B) Minor groove protons. Solid bars, H1′; crosshatched bars, H2′; open bars, H2″. (C) Exchangeable protons. Solid bars, G N1H or T N3H. (D) Phosphates. $\Delta\delta = [\delta_{\text{modified oligodeoxynucleotide}} - \delta_{\text{unmodified oligodeoxynucleotide}}]$ (ppm). The assignment for $P^7$ was made through H4′ $^{31}$P NMR cross-peaks as unmodified Dickerson dodecamer.[43] The numbering of the phosphate groups in the dodecamer is shown at the bottom.

to the electronegative guanine $O^6$ at base pair $C^3{\cdot}G^{10}$, as predicted from molecular modeling,[8] and assumed to be electrostatic in origin. Figure 7 shows the structure emergent from the rMD calculations. It was a right-handed duplex with the propylammonium group located in the major groove, pointing toward the 3′-direction. All Watson−Crick base pairs remained intact. The calculations predicted that the tethered cationic adduct induced bending.

The $^{31}$P NMR chemical shift perturbation in the 3′-direction at the phosphodiester linkage between nucleotides $C^9$ and $G^{10}$ provided a critical restraint for the rMD calculations. A set of calculations was run, in which only NOE and dihedral angle restraints were included for which no distance restraints were placed on the $\omega$-ammonium group. The final averaged structure from this set of calculations was a right-handed duplex with the $\omega$-aminopropyl group floating in the major groove, pointing toward the 3′-direction. In this structure, the $\omega$-aminopropyl group caused minimal distortion in the DNA duplex. All Watson−Crick base pairs remained intact. However, this structure did not predict bending of the DNA duplex.

The precision of the rMD-calculated structures was determined by pairwise rmsd measurements. There were sufficient restraints to ensure satisfactory convergence of the calculations,

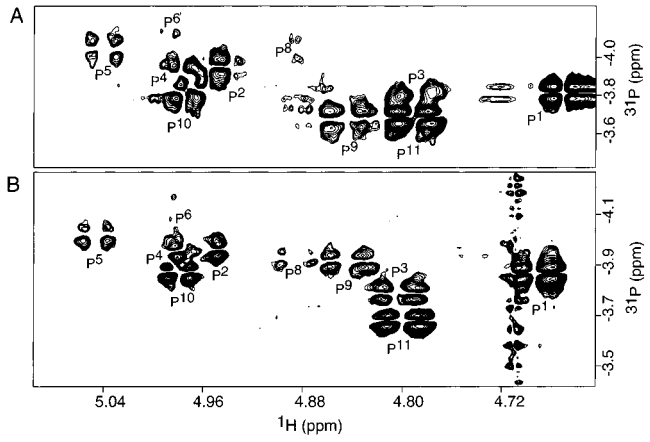


***Figure 6.*** H3′ region of (A) selective excitation $^{31}$P−$^{1}$H COSY spectrum of Dickerson dodecamer and (B) nonselective excitation $^{31}$P−$^{1}$H COSY spectrum of Z3dU-modified Dickerson dodecamer. Both spectra were collected at 303 K. The collected data matrix for both spectra was 256 ($t1$) × 2048 ($t2$) complex points. The data were Fourier transformed after zero filling in the $t1$ dimension, resulting in a matrix size of 512 ($D_1$) × 2048 ($D_2$) real points. Solvent suppression function was used for spectrum A. For the numbering of the phosphate groups and assignment of $P^7$, see Figure 5 legend.

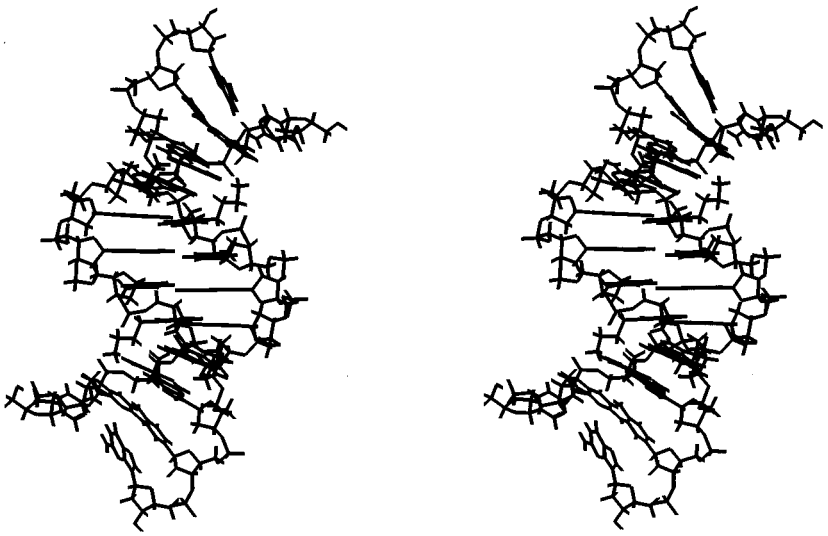

***Figure 7.*** Stereoview showing the average structure of the Z3dU-modified dodecamer emergent from the rMD calculations.

***Table 1.*** Analysis of the MD-Generated Structures of the Z3dU-Modified Dodecamer by X-PLOR

| | |
|---|---|
| NMR Restraints | |
| total no. of distance restraints | 652 |
| interresidue distance restraints | 232 |
| intraresidue distance restraints | 360 |
| DNA−Z3dU distance restraints | 40 |
| Z3dU−Z3dU distance restraints | 20 |
| H-bonding restraints | 32 |
| dihedral planarity restraints | 24 |
| sugar pucker restraints | 120 |
| backbone torsion angle restraints | 90 |
| Structural Statistics | |
| NMR *R*-factor ($R_1^x$)[a] | |
| ⟨rMDRi⟩ | 0.0784 ± 0.0007 |
| rmsd of NOE violations (Å) | 0.00567 ± 0.00001 |
| no. of NOE violations >0.2 Å in the entire duplex | 0 |
| root-mean-square deviations from ideal geometry | |
| bond length (Å) | 0.01105 ± 0.00006 |
| bond angle (deg) | 2.079 ± 0.007 |
| improper angle (deg) | 0.56 ± 0.02 |
| pairwise rmsd (Å) over all atoms | |
| ⟨rMDRi⟩ vs ⟨rMDav⟩ | 0.61 ± 0.04 |

[a] Only the inner 10 base pairs were used in the calculations, to exclude end effects. The mixing time was 250 ms. All values for $R_1^x$ are $\times 10^2$. $R_1^x = \sum|(a_o)_i^{1/6} - (a_c)_i^{1/6}|/\sum|(a_o)_i^{1/6}|$, where $a_o$ and $a_c$ are the intensities of observed (nonzero) and calculated NOE cross-peaks. ⟨rMDRi⟩, 12 converged structures starting from either ZdU-A or ZdU-B; ⟨rMDav⟩, average of 12 converged structures.

irrespective of starting structure. Moreover, the calculations in which the $\omega$-aminopropyl group was either required to be proximate to $G^{10}O^6$ or not required to be proximate to $G^{10}O^6$ both resulted in a maximum pairwise rmsd of <1 Å.

The accuracy of the emergent structures was assessed by complete relaxation matrix calculation.[13] Both sets of calculations, for which the $\omega$-aminopropyl group was either required to be proximate to $G^{10}O^6$ or not required to be proximate to $G^{10}O^6$, satisfied experimental NOE data. The overall value of the sixth root residual $R_1^x$ for the bent structure shown in Figure 7 was $8.7 \times 10^{-2}$. The structural statistics are shown in Table 1.

## Discussion

The incorporation of the cationic Z3dU moiety into the Dickerson dodecamer provided a basis for examining conformational alterations of the double helix induced by site-specific modulation of DNA electrostatics. It provided a model for understanding how electrostatics modulate the reactivity of the double helix to site-specific alkylating agents. The data suggested that this tethered cation oriented in the major groove in the 3′-direction from the modified base and did not perturb Watson−Crick base pairing. The data also suggested that, in this dodecamer, charge neutralization induced by site-specific placement of the ammonium group resulted from the cation being proximate to the floor of the major groove at $G^{10}O^6$ and consequently induced DNA bending.

**Major Groove Orientation of the Tethered Cation.** A number of lines of spectroscopic evidence supported the conclusion that the $\omega$-aminopropyl group oriented in the major groove and faced in the 3′-direction from the modified nucleobase. The sequential NOE connectivities for base steps were observed for all bases. No NOE peaks exhibited unusual intensities. Likewise, the expected NOE connectivities between Watson−Crick hydrogen-bonded imino protons of the ZdU-modified dodecamer were observed. The observation of the imino resonance of the Z3dU nucleotide $X^8$ indicated that this nucleotide was Watson−Crick hydrogen-bonded and inserted into the helix. The NOE data were corroborated by chemical shift data showing that the $^1$H NMR spectrum of the modified dodecamer was similar to that of the unmodified dodecamer.[20,24] Significant deviations for $^1$H NMR chemical shifts were not observed, including protons on the modified base $X^8$. This was consistent with the observation that the cationic Z3dU residue had little effect on the $T_m$ of the modified dodecamer, as compared to that of the unmodified oligodeoxynucleotide. A similar result was noted from detailed thermodynamic studies of Z3dU incorporated into a DNA hairpin.[25]

**DNA Bending.** The site-specific perturbation of the $^{31}$P NMR chemical shift, located in the 3′-direction at the phosphodiester linkage between nucleotides $C^9$ and $G^{10}$, provided evidence for the conclusion that the modified dodecamer was bent. The $^{31}$P NMR chemical shift perturbation was consistent with potential energy minimization calculations carried out by Dande et al.[8] These predicted that the tethered cationic ammonium

(25) Soto, A. M.; Kankia, B. I.; Dande, P.; Gold, B.; Marky, L. A. *Nucleic Acids Res.* **2001**, *29*, 3638−3645.

group was located on the floor of the major groove adjacent to the $O^6$ position of deoxyguanosine. This, in combination with the $^{31}P$ NMR data, provided the rationale for inclusion of the restraint placing the cationic ammonium group proximate to $G^{10}O^6$.

Evidence from other laboratories supported the assertion that site-specific incorporation of the tethered aminopropyl cationic moiety into the major groove of the duplex resulted in bending. The binding of cationic amino acids to the major groove was simulated by ammonium cations tethered on propyl and hexyl linkers by Maher and co-workers. Analysis of electrophoretic mobility patterns demonstrated that the DNA bent toward the neutralized major groove.[5,6] This was in accord with a model in which the cation site-specifically neutralized the negatively charged phosphodiester backbone, leading to the collapse of the backbone toward the cation, consistent with calculations.[2] Fluorescence resonance energy-transfer experiments conducted independently on a related 14-mer duplex were consistent with Z3dU-induced helical bending (Parkhurst, L. J.; Parkhurst, K. M.; Williams, S. L., personal communication). These data showed a decreased 5′-dye to 3′-dye distance for the aminoalkyl-modified duplex, relative to that for the unmodified duplex, that corresponded to DNA bending.[26]

**Structural Basis for DNA Bending.** Dande et al.[8] proposed that the $\omega$-aminoalkyl side chain was positioned in the 3′-direction on the floor of the major groove. In their model, the localized cation repulsed free cations associated with the phosphate backbone. The resulting "naked" phosphates collapsed onto the major groove localized cation, similar to the Rouzina and Bloomfield[10] model. Support for the Dande et al.[8] hypothesis was provided by thermodynamic studies of Soto et al.[25] Thermodynamic measurements of Z3dU incorporated into 5′-d(CGTAGXCGTGC-3′•5′-d(GCACGACTACG)-3′ revealed that the increased stability of the modified duplex was entropy driven. This was attributed to electrostatic effects associated with a localized bend.[27] The Dande et al. molecular modeling studies[8] were supported by nanosecond time scale molecular dynamics simulations of solvated oligodeoxynucleotides with counterions.[28−33] Recent studies suggested preferential cation binding at the floor of the major groove adjacent to the edges of G•C base pairs close to the G $O^6$ and G N7 positions. These cations exhibited significant residence lifetimes on the order of 500 ps.[32]

Crystallographic data of the dodecamer at higher atomic resolution than in the original experiments[34−39] provided additional insight into the intrusion of cations into electronegative regions at the floors of the DNA grooves. Early reports of monovalent cations localized in the grooves of DNA[38,39] were controversial.[36] Recent studies with monovalent ions used anomalous scattering methods.[40] Howerton et al.[37] suggested partial occupancy of $Tl^+$ binding sites located within the major groove of the Dickerson dodecamer. Cation binding was observed at the major groove edge of G•C pairs, adjacent to the guanine $O^6$ and N7 positions.[37] The crystallographic data involving $Tl^+$ counterions in the major groove[37] were consistent with the calculated high electronegative potential associated with the floor of the major groove.[41] The $Tl^+$ data corroborated computational studies which predicted that cations should exhibit significant residence times in the major groove adjacent to the guanine N7 and $O^6$ positions.[32]

The localization of the $^{31}P$ NMR chemical shift perturbation at the phosphodiester linkage between nucleotides $C^9$ and $G^{10}$ was distal to the modified base pair $A^5$•$X^8$. It was not expected that accommodation of Z3dU would require structural distortion at this locus. However, NOE data showed that the cationic ammonium group was oriented in the 3′-direction. This suggested that the chemical shift perturbation at the phosphodiester linkage between nucleotides $C^9$ and $G^{10}$ might have arisen from a site-specific neutralization of negative electrostatic potential in the major groove at this site. Such an interaction was suggested at the same positions[8,11] on the basis of electrostatic footprinting studies. The rMD calculations predicted that placing the ammonium group proximate to the electronegative center at $G^{10}O^6$ required the Z3dU-modified dodecamer to bend. This allowed the propyl moiety to extend its reach to base pair $C^3$•$G^{10}$ (Figure 7).

Back-calculation of NOEs using the bent duplex indicated that the predicted bending was consistent with the spectroscopic data. Restrained molecular dynamics calculations carried out without restraining the Z3dU proximate to $G^{10}O^6$ showed the Z3dU cationic side chain positioned in the 3′-direction but did not predict bending of the DNA duplex. However, in the absence of additional restraints, $^1H$ NOE data and dihedral torsion angle data for deoxyribose sugars typically do not provide reliable indicators of bending. The present data do not differentiate whether the tethered cation introduces a static bend into the duplex, or if instead the duplex is in rapid equilibrium on the NMR time scale between bent and nonbent conformations. The latter situation might arise if the cationic binding site adjacent to base pair $C^3$•$G^{10}$ were only fractionally occupied by the ammonium ion. The cation examined in the present work differs from a free cation in that it is tethered. Consequently, its fractional occupancy of a cationic binding site at base pair $C^3$•$G^{10}$ could be quite high as compared to that of a free cation. This, in turn, would be consistent with the chemical footprinting studies showing regioselective inhibition of guanine N7 methylation by *N*-methyl-*N*-nitrosourea (MNU).[8,9]

Maher et al. proposed that phosphodiester neutralization resulted from salt-bridge formation between the cationic aminopropyl group and the phosphodiester backbone.[4,5,7] Our data

(26) Wu, J.; Parkhurst, K. M.; Powell, R. M.; Brenowitz, M.; Parkhurst, L. J. *J. Biol. Chem.* **2001**, *276*, 14614−14622.
(27) Mikhailopulo, I. A.; Poopeiko, N. E.; Pricota, T. I.; Sivets, G. G.; Kvasyuk, E. I.; Balzarini, J.; De Clercq, E. *J. Med. Chem.* **1991**, *34*, 2195−2202.
(28) Beveridge, D. L.; McConnell, K. J. *Curr. Opin. Struct. Biol.* **2000**, *10*, 182−196.
(29) Hamelberg, D.; McFail-Isom, L.; Williams, L. D.; Wilson, W. D. *J. Am. Chem. Soc.* **2000**, *122*, 10513−10520.
(30) Hamelberg, D.; Williams, L. D.; Wilson, W. D. *J. Am. Chem. Soc.* **2001**, *123*, 7745−7755.
(31) McConnell, K. J.; Beveridge, D. L. *J. Mol. Biol.* **2000**, *304*, 803−820.
(32) Auffinger, P.; Westhof, E. *J. Mol. Biol.* **2000**, *300*, 1113−1131.
(33) Auffinger, P.; Westhof, E. *J. Mol. Biol.* **2001**, *305*, 1057−1072.
(34) Tereshko, V.; Minasov, G.; Egli, M. *J. Am. Chem. Soc.* **1999**, *121*, 470−471.
(35) Egli, M. *Chem. Biol.* **2002**, *9*, 277−286.
(36) Chiu, T. K.; Kaczor-Grzeskowiak, M.; Dickerson, R. E. *J. Mol. Biol.* **1999**, *292*, 589−608.
(37) Howerton, S. B.; Sines, C. C.; VanDerveer, D.; Williams, L. D. *Biochemistry* **2001**, *40*, 10023−10031.
(38) Shui, X.; McFail-Isom, L.; Hu, G. G.; Williams, L. D. *Biochemistry* **1998**, *37*, 8341−8355.
(39) Shui, X.; Sines, C. C.; McFail-Isom, L.; VanDerveer, D.; Williams, L. D. *Biochemistry* **1998**, *37*, 16877−16887.
(40) Soudeyns, H.; Yao, X. J.; Gao, Q.; Belleau, B.; Kraus, J. L.; Nguyen-Ba, N.; Spira, B.; Wainberg, M. A. *Antimicrob. Agents Chemother.* **1991**, *35*, 1386−1390.
(41) Lavery, R.; Pullman, B. *J. Biomol. Struct. Dyn.* **1985**, *2*, 1021−1032.

argue, in this DNA sequence, against the formation of a salt bridge between the ammonium group and the 5′-phosphate of Z3dU.[7,42,43] The refined structures emergent from rMD calculations predicted that the distance from the amino group to the nearest phosphate oxygen was >5 Å. Furthermore, no $^{31}$P NMR chemical shift perturbation was observed for the phosphodiester linkage between nucleotides $T^7$ and $X^8$.

**Summary.** When placed into this dodecamer, the $\omega$-aminopropyl group of Z3dU oriented in the major groove and in the 3′-direction from the modified nucleobase. It was accommodated without perturbation of Watson−Crick base pairing. In this dodecamer, it did not form a salt bridge to the 5′-phosphate of Z3dU. Instead, the tethered cation preferred the floor of the major groove proximate to the deoxyguanosine $O^6$ atom of base pair $C^3$•$G^{10}$. This corroborated chemical footprinting studies, in which DNA methylation by MNU was inhibited regioselectively in the 3′-direction by point substitutions of Z3dU and related zwitterionic residues.[8,9] It corroborated molecular modeling that predicted 3′-orientation of the alkylammonium group due to unfavorable steric interactions in the 5′-direction.[8]

**Acknowledgment.** This work was supported by NIH Grant CA-76049. Funding for the NMR spectrometer was supplied by NIH Grant RR-05805 and the Vanderbilt Center in Molecular Toxicology ES-00267. We thank Mr. Markus Voehler who assisted with NMR experiments.

**Supporting Information Available:** Table S1, which shows the experimental distances and classes of restraints; Tables S2−S5, which detail the $^1$H and $^{31}$P NMR chemical shift assignments; Table S6, which shows partial charge and atom type of Z3dU residue used for X-PLOR calculation; Table S7, which shows helicoidal parameters associated with Figure 7; Figure S1, which shows the distribution of experimental NOE restraints applied in the structural refinement and the per-residue $R_1^x$ values for the X-PLOR-determined structure (PDF). This material is available free of charge via the Internet at http://pubs.acs.org.

JA0201707

(42) Hashimoto, H.; Nelson, M. G. *J. Org. Chem.* **1993**, *58*, 4194−4195.
(43) Hashimoto, H.; Nelson, M. G. *J. Am. Chem. Soc.* **1993**, *115*, 7128−7134.